

Sound Intensity Measurements in Vehicle Interiors

Jakob Mørkholt, Jørgen Hald and Svend Gade, Brüel & Kjær, Nærum, Denmark

In some cases it is important to be able to measure not only the total sound intensity of a panel surface in a vehicle interior, but also the components of that intensity due to sound radiation and absorption of the incident field. These intensity components may be needed for calibration of energy flow models of vehicle interior noise. A robust method based on a surface absorption coefficient measurement is presented in this article.

Consider the radiation of sound from a small surface segment in a cabin environment. Such a surface segment may radiate sound energy because of external forcing, causing the surface to vibrate, and it may absorb energy from an incident sound field because of finite-surface acoustic impedance. When measuring the sound intensity over the surface segment with an intensity probe, the total intensity I_{tot} will be measured. Assuming the radiated field and the incident field to be mutually incoherent, the total intensity is equal to the sum of the radiated sound intensity I_{rad} that would exist with no incident field and the sound intensity component I_{abs} due to absorption from the incident field:

$$I_{tot} = I_{rad} + I_{abs} \quad (1)$$

Considering the intensity in the outward normal direction on the panel surface, the radiated intensity will typically be positive, while the component due to absorption will typically be negative. So for vibrating panels with an absorptive surface, the total measured intensity may be small, although the radiated intensity is relatively high. Often it is of interest to know not only the total intensity but also the components due to radiation and absorption. For example, this kind of information is needed in energy-based modeling that describes the energy flow between subsystems.¹

The method presented here is based on separation of different sound field components via the spatial sound field information provided by an array. The radiated intensity is estimated as the intensity that would exist if the incident and scattered field components could be taken away. So a free-field radiation condition is simulated. The idea is to first separate the incident field component, then use separately measured information about the scattering properties of the panel to calculate the scattered field, and finally subtract the incident and scattered fields from the total sound field. The method needs the panel geometry, which is either imported as a computer-aided design (CAD) model or measured with a 3D digitizer and then uses a measured map of absorption coefficient. The separate measurement of the surface absorption coefficient is done with loudspeaker excitation.

Description of Methodology

The array measurements considered here are cross-spectral measurements of the full cross-spectral matrix between all array microphones, and then a principal component sound field representation based on what is extracted.² As a consequence, no phase information is available between different array positions, so a separate patch holography calculation has to be performed for each position. We used a double layer array (DLA), and the processing was performed using statistically optimized NAH (SONAH).^{3,4} In the following, we will consider only a single principal component; that is, a spatially coherent sound field with coherent sources. We shall use a complex time harmonic representation with the time variation $e^{j\omega t}$ suppressed.

Extraction of the Incident Field. A basic array processing task is that of extracting the incident sound field from the total sound field. Considering the sound field on a small panel segment in a cabin, the distinction between the incident field and the radiated field is, however, not obvious even when we look at the field very

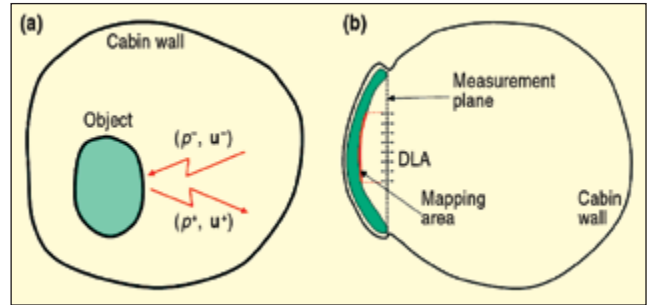


Figure 1. Separation of inward (incident) and outward propagating field components (p^-, \mathbf{u}^-) and (p^+, \mathbf{u}^+); (a) clearly separated sources; (b) smooth transition between sources.

near the panel segment. Because of coherent vibration components and significant mutual radiation impedances between neighboring panel segments, some neighboring segments should be included as sources of the radiated field. Figure 1 illustrates how this distinction can be made in practice with a DLA. Using SONAH holography on a DLA measurement, the sound field components (p^-, \mathbf{u}^-) and (p^+, \mathbf{u}^+) with sources on different sides of the array plane can be separated:^{3,4}

$$(p_{total}, \mathbf{u}_{total}) = (p^-, \mathbf{u}^-) + (p^+, \mathbf{u}^+) \quad (2)$$

The array must then be used in such a way that the pressure p^- and the velocity vector \mathbf{u}^- represent the field incident on the source area of interest, while the outward propagating field component (p^+, \mathbf{u}^+) is the sum of the scattered and radiated fields:

$$(p^+, \mathbf{u}^+) = (p_{sct}, \mathbf{u}_{sct}) + (p_{rad}, \mathbf{u}_{rad}) \quad (3)$$

Figure 1a illustrates the case of an isolated source object, where the incident and outward-propagating field components are well defined. They could be determined, for example, based on measurements across two concentric spherical surfaces that enclose the test object. Figure 1b illustrates the case of measurement with a DLA on a panel section in a vehicle interior. Here, the measurement plane will define the distinction between sources of the incident field and sources of the outward propagating field. But the distinction will not be sharp due to the limited angular resolution of a practical array.

Solution to Scattering Problem. Provided the incident and radiated fields are mutually incoherent, then Equation 1 is the basis for a simple and robust energy based method. The basic assumption is that we can measure a local absorption coefficient α at each point \mathbf{r} on the source surface so that that the normal components I^- and I_{abs} of the incident and absorbed intensities are related by:

$$I_{abs}(\mathbf{r}) = \alpha(\mathbf{r})I^-(\mathbf{r}) \quad (4)$$

In general, the ratio $I_{abs}(\mathbf{r})/I^-(\mathbf{r})$ between the two intensities will depend on the form of the incident field. However, if the coefficient $\alpha(\mathbf{r})$ is measured with an incident field that is sufficiently similar with the incident field under operational conditions, then Equation 4 can provide good results with the operational field.

The method requires a separate set of DLA measurements with artificial speaker excitation. Figure 2 illustrates a setup with a set of incoherently excited speakers to create an incident field similar to the field incident under flight conditions in an aircraft. As noted previously, the DLA/SONAH measurement can provide the total and incident components of the loudspeaker-generated sound field on the panel surface. Since in this case, the absorbed intensity is equal to the total intensity, then in accordance with Equation 4, the absorption coefficient is calculated as the ratio between the total

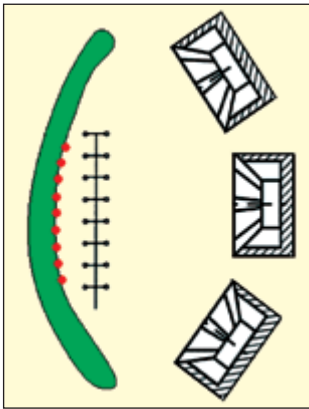


Figure 2. Cabin panel section with surface calculation points covered by specific array position; speakers for measurement of surface properties are shown.

responding to different operational conditions.

Once an operational measurement has been taken, the associated total, incident and outgoing field components on the panel surface can be estimated using SONAH. The absorbed intensity is estimated using Equation 4, and the radiated intensity is then obtained using Equation 1.

Measurement

Measurement System. The system for data acquisition is based around the DLA shown in Figure 3. The array has 8 × 8 microphones mounted in two layers, resulting in a total of 128 microphones. The microphones are spaced 30 mm apart in both directions and with a spacing of 31 mm between the two layers. This results in an upper frequency limit for the array of 5.7 kHz (spatial sampling limit).

Also mounted on the array are six infrared LEDs that are used in connection with a position measurement system monitoring the array position and orientation on line. This system is based around an integrated camera unit. The camera unit has three built-in line cameras that determine LED positions. The camera unit is connected to a controller box that again communicates with a PC via an RS-232 port. The LEDs on the array are also connected to this controller box. The position measurement system also has associated with it a wireless pointing device for measuring 3D point positions. This device can be used in connection with the measurement software to record 3D position data on the surfaces under investigation.

The DLA is connected to two 65-channel front ends that are again connected to the controlling PC via a LAN. A third front end with generator units is used for driving artificial excitation speakers through power amplifiers.

The controlling PC runs measurement software with a dedicated measurement template for acquiring array microphone signals and corresponding array positions in space as well as surface point position data. As outlined above, the analysis method requires a model of the surfaces to be analyzed. Such a model can either be imported from a CAD model or digitized on the spot. Digitizing involves point measurements as outlined above, followed by curve and surface construction. In both cases, the end result is a CAD-type parametric surface description that is later used as the basis for creating a surface mesh. This mesh is in turn used for calculation and results display.

Measurement Procedure. The DLA is placed in positions close to the surfaces under investigation to sample the near-field sound pressure. The position of the array is recorded online via the position measurement system and microphone time histories are recorded for each array position. The array is placed in slightly overlapping positions to cover the investigated surfaces patch by patch. The data acquisition software displays the position of current and past array positions in 3D along with the surface model. This way the user can identify those parts of the surface that have been covered with the array and those that still need to be covered.

and the incident intensities. Accurate measurement of the array positions relative to the panel geometry using an integrated position measurement system allows the admittances and absorption coefficients to be calculated at predefined points on the panel surface (see Figure 2).

For the case of a car cabin application, the surface property measurement will typically be performed with the car not in motion, while the operational measurement will be performed while driving. Often, a single surface property measurement will be applied with several operational measurements, corresponding to different operational conditions.

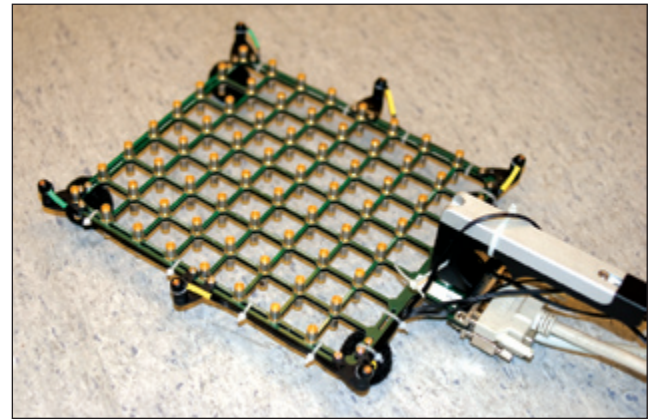


Figure 3. Double-layer array (DLA) mounted with six IR LEDs.

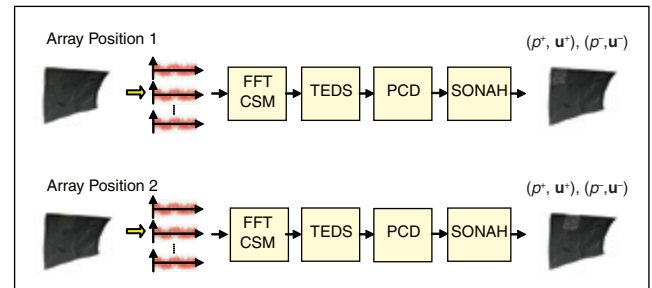


Figure 4. Processing steps for each array position.

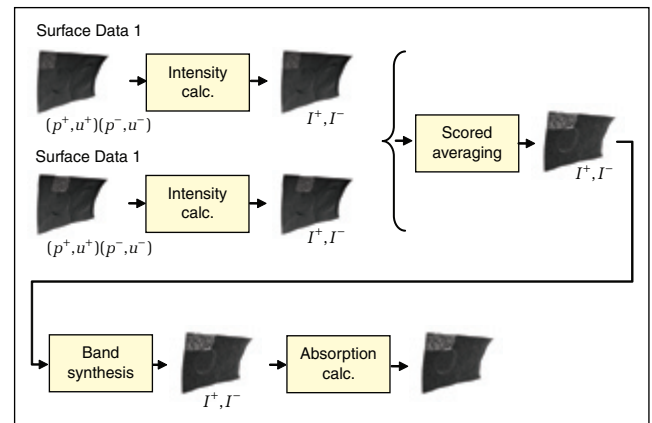


Figure 5. Processing for absorption coefficient estimation.

When measuring for the estimation of surface absorption, a number of loudspeakers are distributed in the cabin interior and driven by uncorrelated noise sources to create a distributed and (close-up) diffuse excitation field. Measurement for the actual estimation of entering intensity is performed in operating conditions with these sources turned off. All recorded data are stored to a database.

Data Processing. The post-processing software application retrieves all data from the database. A surface mesh is created based on the parametric surface description. A number of mesh areas may be defined in this process. These can be used for averaging of an absorption coefficient, for example.

The time histories measured in each array position are processed as shown in Figure 4. First the full cross spectral matrix (CSM) for all signals is calculated by FFT and the frequency responses corrected with response correction data from the individual microphones (TEDS). Then a principal component decomposition (PCD) is performed to determine the most significant incoherent components. Each component is finally processed via SONAH to determine corresponding incoming and outgoing sound field quantities on the source surface.

From this point on, the processing depends on the quantity to be determined. The case of absorption coefficient estimation is illustrated in Figure 5. Based on the partial sound field quantities, the total incoming and outgoing surface intensity components are

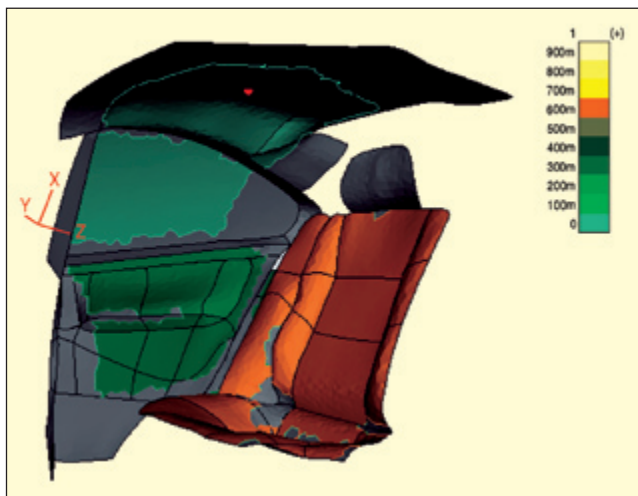


Figure 6. Contour plot of estimated absorption coefficient of seat, door, window and roof in car cabin; results shown for 200-Hz, 1/3-octave band. (results averaged also over respective areas).

calculated for surface points corresponding to each array patch. Results from different patches are then averaged on the surface mesh using a scoring method. Each mesh node-to-array position combination is assigned a score depending on how the node is positioned relative to the array. If more than one array contributes to a node, the results for that node are averaged using the scores. This way, a contribution estimated with a “well-positioned” array will be given more weight in the averaging. The surface intensity values are then band synthesized into one-third octave bands, for example, and optionally averaged over pre defined averaging areas. Finally, the absorption coefficient is estimated in each node using Equation 4.

Mapping of Absorption Coefficient in a Car Cabin. To illustrate the use of the proposed techniques in an automotive application, measurements were made with the DLA system in the interior of a Volvo S60 passenger car to determine *in-situ* absorption coefficient of selected surfaces in the cabin. First, the cabin surfaces to be investigated were digitized using the 3D position measurement system and dedicated digitizing software. Next, array measurements were made with the DLA covering the surfaces patch by patch. Four loudspeakers were distributed in the cabin and driven by white noise to provide the acoustic excitation needed for estimating the absorption coefficient

Figure 6 shows a 3D contour plot of the estimated absorption coefficient on the cabin surfaces for the 200-Hz, 1/3-octave band. The absorption coefficient was estimated by first doing 1/3-octave-band synthesis of the estimated total and incident intensities, and then doing area averaging of these quantities over a seat or window surface, for example, before estimating the final absorption coefficient as the ratio between the two. The figure shows that in the 200-Hz frequency band, the seat has quite a high absorption coefficient compared to the door, window and roof.

Figure 7 shows the estimated average absorption coefficients in 1/3-octave bands for the roof (A), the seat (B) and the window (C). The roof was covered by a thin layer of foam material that could be expected to have an absorption coefficient increasing with frequency as the graph shows. The seat shows an absorption coefficient decreasing with frequency, which could be explained by the seat material being a leather type of material that is probably acoustically “hard” at higher frequencies. Finally, the window shows quite a low absorption coefficient throughout the whole frequency range under investigation, as could be expected.

Conclusions

A method for measuring the absorption coefficient, radiated and absorbed intensity on the panels of a vehicle interior has been described. We showed how the method can be used to map the absorption coefficient on the interior surfaces of a car cabin. The method is based on a dual-layer array with integrated position measurement.

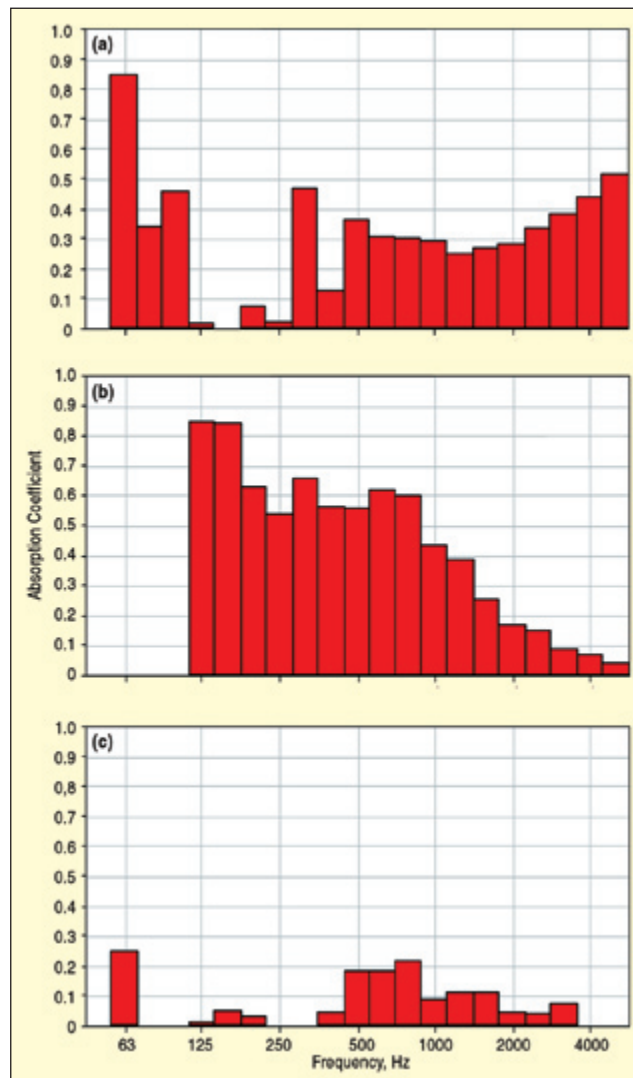



Figure 7. Estimated absorption coefficient on roof, seat and window of car cabin as functions of frequency (results shown in 1/3-octave bands).

Acknowledgement

This article is based on work done in the European Union research project Cabin Noise Reduction by Experimental and Numerical Design Optimization (CREDO), which deals with noise in aircraft and helicopter cabins. Since the radiated intensity is often seen from the perspective of the cabin, it is sometimes also called entering intensity (EI).⁴ Simulations as well as results of measurements inside aircraft are found in References 4 and 7.

References

1. P. Hardy, D. Trentin, L. Jézéquel and M. N. Ichchou; “Identification of Noise Sources in an In-Flight Aircraft by Means of Local Energy Method,” *Proceedings of Euronoise 2006*.
2. J. Hald, “STSF – A Unique Technique for Scan-Based Near-field Acoustical Holography without Restrictions on Coherence,” *Brüel & Kjær Technical Review*, No. 1, 1989.
3. J. Hald; “Patch Holography in Cabin Environments Using a Two-Layer Hand-Held Array with an Extended SONAH Algorithm,” *Proceedings of Euronoise 2006*.
4. J. Hald and J. Mørkholt; “Methods to Estimate the Entering Intensity and their Implementation Using SONAH,” Report DWP2.3 from the European project CREDO, 2007.
5. J. D. Alvarez and F. Jacobsen; “*In-Situ* Measurements of the Complex Acoustic Impedance of Porous Materials,” *Proceedings of Inter-Noise 2007*.
6. J. Hald, J. Mørkholt; “Array-Based Measurement of Radiated and Absorbed Sound Intensity Components,” *Proceedings of Acoustics 2008*.
7. J. Hald, J. Mørkholt, P. Hardy, D. Trentin, M. Bach-Andersen and G. Kieth, “Measurement of Absorption Coefficient, Surface Admittance, Radiated Intensity and Absorbed Intensity on the Panels of a Vehicle Cabin using a Dual Layer Array with Integrated Position Measurement,” *Proceedings of SAE*, 2009. 

The author may be reached at: sgade@bksv.com.